

## A FINITE ELEMENT MODEL FOR PLAIN WEAVE FABRICS BASED ON AN INNER BEAM STRUCTURE

Benjamin Kaiser<sup>1</sup>, Thomas Pyttel<sup>2</sup>, Eberhard Haug<sup>3</sup>, Fabian Duddeck<sup>4</sup>

<sup>1</sup>Technische Hochschule Mittelhessen, Friedberg, Germany

Email: benjamin.kaiser@m.thm.de, Web Page: <http://www.m.thm.de/m>

<sup>2</sup>Technische Hochschule Mittelhessen, Friedberg, Germany

Email: thomas.pyttel@m.thm.de, Web Page: <http://www.m.thm.de/m>

<sup>3</sup>ESI Group, Aix en Provence, France

Email: eberhard.haug@esi-group.com, Web Page: <http://www.esi-group.com>

<sup>4</sup>Technische Universität München, München, Germany

Email: duddeck@tum.de, Web Page: <http://http://www.tum.de>

**Keywords:** draping, woven fabrics, coupled multiscale, finite element, textile composites

### Abstract

The paper presents a finite shell element for plain weave fabrics. It is designed for draping and forming simulations. Instead of a classical constitutive law, a unit cell is modeled with crossed beams. With that approach, it is possible to describe the kinematics of the fibers in a natural way.

The structure of the unit cell is presented. The setup of the system of equations for the unit cell and the formulation of the boundary conditions is explained. The nonlinear problem is solved with a Newton iteration. Shearing is not considered in the unit cell. Hence shearing effects are taken into account via a so-called parent sheet. Based on these assumptions, the membrane behavior of the element is described. Bending behavior is calculated with the Mindlin plate theory. Due to the separate treatment of in plane and out of plane behavior, the bending characteristic is decoupled from tension/compression. The unit cell model is implemented in the user material environment of the industrial explicit FE program PAM-Crash. The presented work is related to draping, but the method offers new opportunities for any application where the inner structure of a material plays an important role.

### 1. Introduction

Traditional methods for the simulation of the draping behavior of woven fabrics are the kinematic and finite element based method [1]. The kinematic method is based on the pin-joint technique where fibers are rigid and cross over points modeled with joints [2] [3]. Advantages of this approach are the simplicity and the high speed of calculation, which makes it attractive for industrial application. Results maybe unprecise because of the rigidity of fibers [4].

For the FE based draping simulation, explicit FE-programs like PAM-Crash, LS-Dyna und Abaqus are used. The fabric is modeled with shell or membrane elements which are following an anisotropic continuum mechanical material law [5] [6] [7] [8]. Material properties have to be homogenized. The kinematic of the fibers is not taken into account.

The presented finite element model combines both methods. It describes the kinematic of the fibers and in addition the fibers are deformable. It is implemented in the standard explicit FE-programs PAM-Crash. A first membrane model like this was presented by [9] for an implicit FE-solver and by [10] an explicit solver.

## 2. Material Law

In order to calculate stresses based on strains, a separate treatment for bending and for membrane behavior is introduced. The bending stress  $\sigma^b$  is calculated with  $\epsilon^b$  by using Mindlin plate theory. For the shear part of the membrane behavior, stress  $\sigma^{m,s}$ , HOOKE'S law is applied. The remaining membrane part represents the mechanical behavior of the fibers of the fabric. This remaining part is modeled by an appropriate unit cell and delivers the stress  $\sigma^{m,uc}$  based on  $\epsilon^{m,uc}$ . The total Cauchy stress  $\sigma$  in the shell element is the sum over

$$\sigma = \sigma^b + \sigma^{m,s} + \sigma^{m,uc} \quad . \quad (1)$$

### 2.1. Unit cell model

The inner unit cell is embedded in a deformed 4 node shell element shown in Figure 1. Warp and weft fiber directions are pointing in the directions of the convected base vectors  $\vec{a}_1$  and  $\vec{a}_2$ , which are tangential to the material related coordinate lines  $\Xi_1$  and  $\Xi_2$ . The warp fiber is pictured in red and the weft fiber in green. The light blue element is responsible for the treatment of the contact between warp and weft fiber.

In Figure 2, the unit cell from Figure 1 is shown. The difference between the two pictures is that

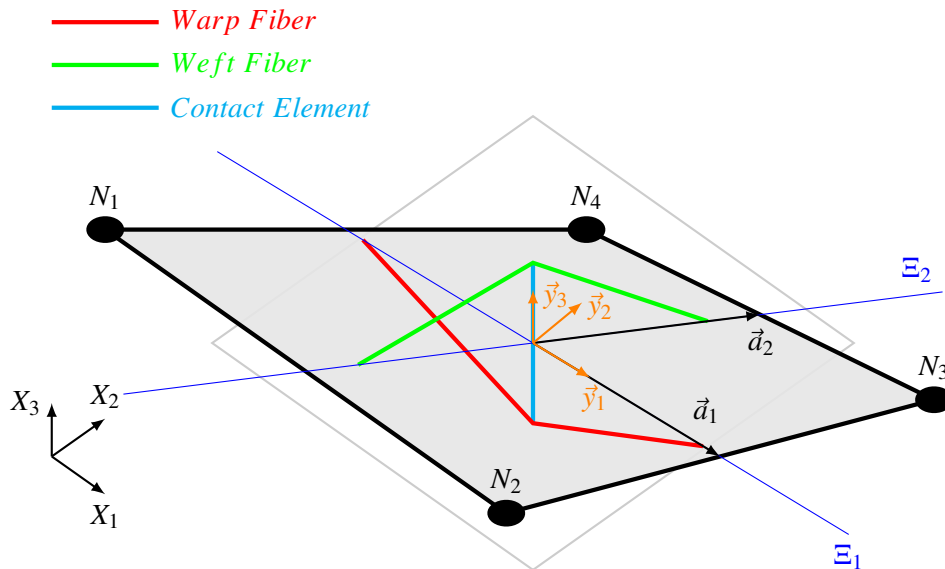


Figure 1: 4-Node shell element with inner structure

in Figure 2 warp and weft fibers are plotted in one plane. In addition, the boundary conditions and the forces  $F_{warp}$  and  $F_{weft}$  are shown. The nodes  $N_1$  and  $N_2$  are loaded with displacements which are calculated based on the membrane strain  $\epsilon^{m,uc}$  of the shell element. The unit cell is modeled with three beam elements. Because of symmetry, only half of the unit cell is modeled. The warp fiber is modeled with beam element 1, the weft fiber is modeled with beam element 2 and the contact between the fibers

is represented by beam 3.

Due to large deformations, the behavior of the mechanical system shown in Figure 2 is nonlinear.

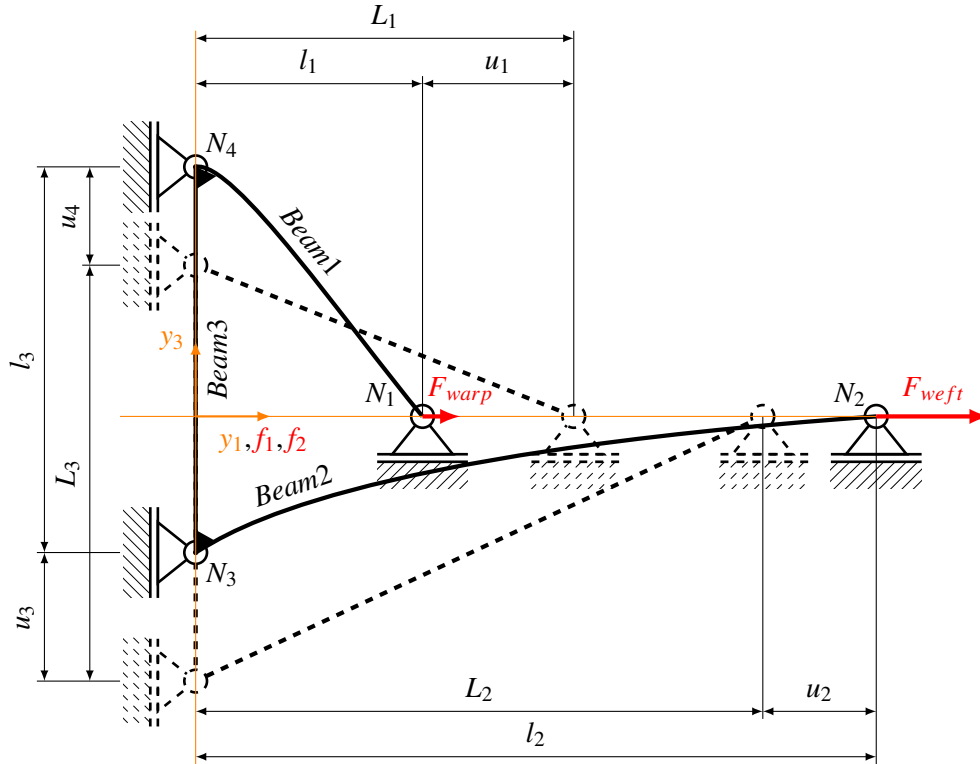


Figure 2: Discrete mechanical system

Therefore, the global stiffness matrix  $K$  contains the elastic part  $K_E$  and the geometrical part  $K_G$

$$K = K_E + K_G \quad . \quad (2)$$

For the formulation of the global stiffness matrix,  $K$ , the following parameters are used:

- Young's modulus of fibers  $E_{warp}$  and  $E_{weft}$
- Young's modulus of contact element  $E_3$
- second moment of inertia of fibers  $I_{warp}$  and  $I_{weft}$
- cross-sections of the fibers  $A_{warp}$  and  $A_{weft}$
- dimensions of the unit cell  $L_1, L_2, L_3$ .

After the introduction of the boundary conditions, the system of equations has the following form

$$\begin{pmatrix} F_{warp} \\ F_{weft} \\ 0 \\ 0 \end{pmatrix} = \begin{pmatrix} K_{11} & K_{12} & K_{13} & K_{14} \\ K_{21} & K_{22} & K_{23} & K_{24} \\ K_{31} & K_{32} & K_{33} & K_{34} \\ K_{41} & K_{42} & K_{43} & K_{44} \end{pmatrix} \cdot \begin{pmatrix} u_1 \\ u_2 \\ u_3 \\ u_4 \end{pmatrix} \quad . \quad (3)$$

The system of equations is nonlinear and is solved iteratively with NEWTON's method. With the computed forces  $F_{warp}$  and  $F_{weft}$ , the stress  $\sigma^{m,uc}$  can be calculated as explained in [10].

## 2.2. Shear

Shear is modeled by a linear relation between coordinates of the Green Lagrange strain tensor  $E_{ij}$  and the coordinates of the 2nd Piola Kirchhoff stress (PK)  $S_{ij}$  in the following form

$$\begin{pmatrix} S_{11} \\ S_{22} \\ S_{12} \end{pmatrix} = \begin{pmatrix} 0 & 0 & 0 \\ 0 & 0 & 0 \\ 0 & 0 & G_{12} \end{pmatrix} \cdot \begin{pmatrix} E_{11} \\ E_{22} \\ E_{12} \end{pmatrix} . \quad (4)$$

The constant shear modulus is  $G_{12}$ . The strain  $E_{ij}$  can be calculated from  $\epsilon^{m,s}$ . Finally, the 2nd PK stress  $S$  is transformed to Cauchy stress  $\sigma^s$ .

## 2.3. Bending

The Mindlin plate theory, described in [11], is used for modeling the bending behavior. The constitutive model inside this theory is a plane stress relation between Cauchy stresses  $\sigma^b$  and logarithmic strains  $\epsilon^b$ . Due to the decoupling of membrane and bending behavior, the  $\epsilon^b$  is calculated from total strain  $\epsilon$  as follows

$$\epsilon^b = \epsilon - \epsilon^m. \quad (5)$$

In order to complete the set of equations,  $\sigma^b$  is computed from

$$\begin{aligned} \sigma_{11}^b &= \frac{E}{1-\nu^2} (\epsilon_{11}^b + \nu \cdot \epsilon_{22}^b) \\ \sigma_{22}^b &= \frac{E}{1-\nu^2} (\epsilon_{22}^b + \nu \cdot \epsilon_{11}^b) \\ \sigma_{12}^b &= G \cdot \epsilon_{12}^b \\ \sigma_{13}^b &= G \cdot \epsilon_{13}^b \\ \sigma_{23}^b &= G \cdot \epsilon_{23}^b . \end{aligned} \quad (6)$$

## 3. Results

As test case for the validation of the unit cell model, a double-dome test is chosen. The FE mesh for the tool is taken from a double-dome benchmark, which has been performed by several labs, shown at <http://www.wovencomposites.org>, in order to validate and compare different approaches. In the publications [12] and [13], a draping experiment was done with the same tool geometry. Experimental results are taken from these publications. The used plain weave fabric in the experiment was a Twintex TPEET22XXX. The material properties of that fabric were studied in the publications [14] and [15]. The specimen size is 470 mm x 270 mm. In the simulation, only a quarter is simulated because of symmetry reasons.

The simulation results of the unit cell model from the double-dome test are shown in Figure 3. On the left side of Figure 3, the simulated material draw-in of the fabric is compared with the material draw-in of the experiment [12]. The green line represents the material draw-in of the experiment. Comparing the green line with the simulated material draw-in, only small differences can be found at the corners. Thus, the material draw-in can be well predicted with the unit cell model. At the right side of Figure 3, the fiber direction and the points for the shear angle measurements are shown. The points from 1 to 10 are on a line of the initial specimen from the point (0, 235) to (135, 0). Point 1 and 10 are on the border of

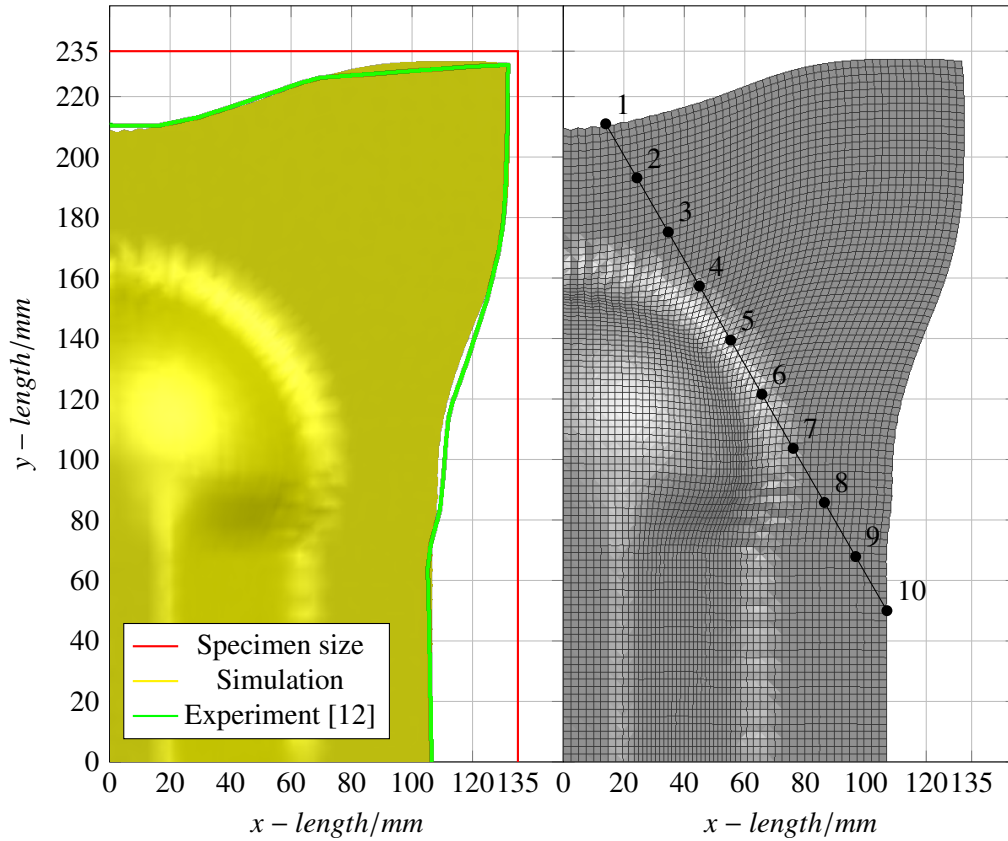


Figure 3: Double dome test - experiment vs. simulation

the deformed part. The line segment from point 1 to 10 is divided in 9 even parts to build point 2 to 9. The shear angle of the experiment and the simulation is compared in diagram 4. The characteristics of

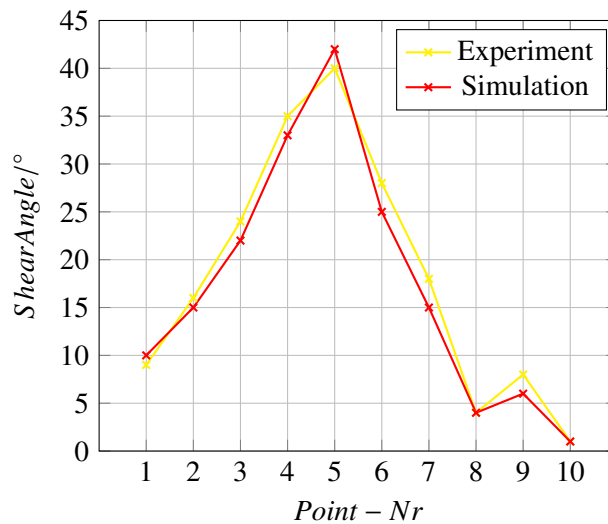


Figure 4: Shear angle - experiment vs. simulation

the curves from experiment and simulation are similar. Remarkable is that the high shear deformation at

point 5 can be captured by the model as well as a lower peak at point 9.

In addition, the simulation of a gravity test with a hemisphere, shown in Figure 5, was done in order to check the plausibility of the model. A woven fabric is loaded with gravity. In Figure 5a, the initial state of simulation is shown. The results of the simulations are represented in Figure 5b and Figure 5c. Figure 5b represents the test with low bending stiffness and with high shear stiffness and Figure 5c represents the test with high bending stiffness and low shear stiffness.

Observing results, Figure 5b shows small shearing deformations with significant wrinkles at the side of the fabric and Figure 5c illustrates large shearing deformations with also significant wrinkles but with different distribution and magnitude. Notably, the model is reacting sensitive to changes of the material properties for shearing and bending. Concluding, wrinkling is well predicted with the different configurations for shearing and bending.

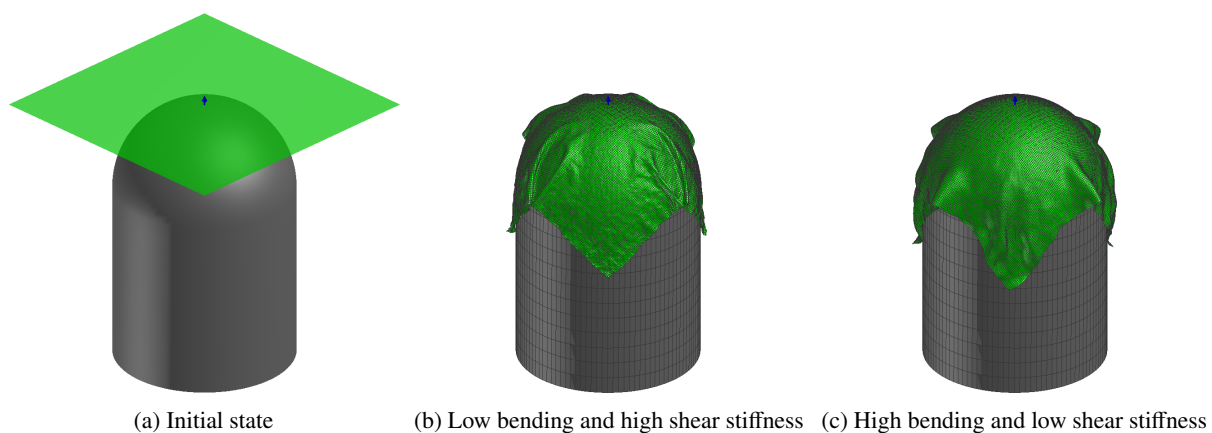


Figure 5: Simulation of draping over hemisphere

#### 4. Conclusion

Draping problems can be solved with a coupled multi-scale approach. For the implemented unit cell, for plain weave fabrics, the approach delivers good results. Draw-in of the fabric sheet while draping can be reproduced. Also the shearing between the fibers can be predicted. The model is sensitive for shearing and bending, which are the basic mechanisms in wrinkling prediction as shown in the examples.

In a next step, the coupling between the inner structure and the shell element will be generalized for periodic fabric materials. Coupling of arbitrary representative unit cell models will be possible. The presented work is related to draping, but the method offers new opportunities for any application where the inner structure of a material plays an important role.

#### References

- [1] S.B. Sharma and M.P.F. Sutcliffe. A simplified finite element model for draping of woven material. *Composites Part A: Applied Science and Manufacturing*, 35(6):637–643, Jun 2004.
- [2] M.P.F. Sutcliffe, S.B. Sharma, A. C. Long, M. J. Clifford, R. G. Gil, P. Harrison, and C. D Rudd. A comparison of simulation approaches for forming of textile composites. In *5th Int. ESAFORM Conf. on Materials Forming, Krakow, Poland*, 311-314, 2002.
- [3] K. Potter. Beyond the pin-jointed net: maximising the deformability of aligned continuous fibre reinforcements. *Composites Part A: Applied Science and Manufacturing*, 33(5):677 – 686, 2002.

- [4] S.G. Hancock and K.D. Potter. The use of kinematic drape modelling to inform the hand lay-up of complex composite components using woven reinforcements. *Composites Part A: Applied Science and Manufacturing*, 37(3):413 – 422, 2006.
- [5] Ivelin Ivanov and Ala Tabiei. Loosely woven fabric model with viscoelastic crimped fibres for ballistic impact simulations. *International Journal for Numerical Methods in Engineering*, 61(10):1565–1583, 2004.
- [6] Ala Tabiei and Ivelin Ivanov. Computational micro-mechanical model of flexible woven fabric for finite element impact simulation. *International Journal for Numerical Methods in Engineering*, 53(6):1259–1276, 2002.
- [7] ESI Group, 100-102 Avenue de Suffren 75015 Paris FR. *PAM-Crash Solver Reference Manual*, 2013 edition.
- [8] Livermore Software Technology Corporation, P. O. Box 712 Livermore, California 94551-0712. *LS-DYNA KEYWORD USER'S MANUAL*, 2014.
- [9] E. Haug, P. De Kermel, B. Gawenat, and A. Michalski. Industrial design and analysis of structural membranes. In *International Conference on Textile Composites and Inflatable Structures STRUCTURAL MEMBRANES*, Barcelona, Spain, 2007.
- [10] B. Kaiser, E. Haug, T. Pyttel, and F. Duddeck. A multi-scale approach for the simulation of textile membranes. In *VII International Conference on Textile Composites and Inflatable Structures - STRUCTURAL MEMBRANES 2015, Barcelona Spain*, 2015.
- [11] W. Becker and D. Gross. *Mechanik elastischer Körper und Strukturen*. Springer-Verlag, 2002.
- [12] M.A. Khan, T. Mabrouki, E. Vidal-Sall, and P. Boisse. Numerical and experimental analyses of woven composite reinforcement forming using a hypoelastic behaviour. Application to the double dome benchmark. *Journal of Materials Processing Technology*, 210(2):378 – 388, 2010.
- [13] S. Gatouillat, A. Bareggi, E. Vidal-Salle, and P. Boisse. Meso modelling for composite preform shaping - simulation of the loss of cohesion of the woven fibre network. *Composites Part A: Applied Science and Manufacturing*, 54:135–144, 2013.
- [14] J. Cao, R. Akkerman, P. Boisse, J. Chen, H.S. Cheng, E.F. de Graaf, J.L. Gorczyca, P. Harrison, G. Hivet, J. Launay, W. Lee, L. Liu, S.V. Lomov, A. Long, E. de Luycker, F. Morestin, J. Padvoiskis, X.Q. Peng, J. Sherwood, Tz. Stoilova, X.M. Tao, I. Verpoest, A. Willems, J. Wiggers, T.X. Yu, and B. Zhu. Characterization of mechanical behavior of woven fabrics: Experimental methods and benchmark results. *Composites Part A: Applied Science and Manufacturing*, 39(6):1037–1053, 2008.
- [15] J. Launay, G. Hivet, A. V. Duong, and P. Boisse. Experimental analysis of the influence of tensions on in-plane shear behaviour of woven composite reinforcements. *Composites Science and Technology*, 68(2):506 – 515, 2008.